American Mineralogist, Volume 83, pages 1387–1398, 1998

Magnetite from magnetotactic bacteria: Size distributions and twinning

BERTRAND DEVOUARD,[1,*] MIHÁLY PÓSFAI,[1] XIN HUA,[1] DENNIS A. BAZYLINSKI,[2] RICHARD B. FRANKEL,[3] AND PETER R. BUSECK[1]

[1]Departments of Geology and Chemistry/Biochemistry, Arizona State University, Tempe, Arizona 85287-1404, U.S.A.
[2]Department of Microbiology, Immunology and Preventive Medicine, Iowa State University, Ames, Iowa 50011, U.S.A.
[3]Department of Physics, California Polytechnic State University, San Luis Obispo, California 93407, U.S.A.

ABSTRACT

We studied intracellular magnetite particles produced by several morphological types of magnetotactic bacteria including the spirillar (helical) freshwater species, *Magnetospirillum magnetotacticum,* and four incompletely characterized marine strains: MV-1, a curved rod-shaped bacterium; MC-1 and MC-2, two coccoid (spherical) microorganisms; and MV-4, a spirillum. Particle morphologies, size distributions, and structural features were examined using conventional and high-resolution transmission electron microscopy. The various strains produce crystals with characteristic shapes. All habits can be derived from various combinations of the isometric {111}, {110}, and {100} forms. We compared the size and shape distributions of crystals from magnetotactic bacteria with those of synthetic magnetite grains of similar size and found the biogenic and synthetic distributions to be statistically distinguishable. In particular, the size distributions of the bacterial magnetite crystals are narrower and have a distribution asymmetry that is the opposite of the nonbiogenic sample. The only deviation from ideal structure in the bacterial magnetite seems to be the occurrence of spinel-law twins. Sparse multiple twins were also observed. Because the synthetic magnetite crystals contain twins similar to those in bacteria, in the absence of characteristic chains of crystals, only the size and shape distributions seem to be useful for distinguishing bacterial from nonbiogenic magnetite.

INTRODUCTION

Many microorganisms facilitate the deposition or dissolution of minerals (Lowenstam and Weiner 1989; Banfield and Nealson 1997). Minerals formed by bacteria are known to be synthesized in two fundamentally different modes of mineralization. In biologically induced mineralization (BIM; Lowenstam 1981), the biomineralization processes are not controlled by the organisms; mineral particles produced in this manner are formed extracellularly, have a broad size distribution, and lack a consistent, defined morphology (Bazylinski and Moskowitz 1997). Magnetite (Fe_3O_4) can be formed through BIM by iron-reducing bacteria. These microorganisms respire with ferric iron, Fe^{3+}, in the form of amorphous Fe^{3+} oxyhydroxide (Lovley 1991) and secrete reduced iron, Fe^{2+}, that reacts with excess Fe^{3+} oxyhydroxide under anaerobic conditions to form magnetite. Thus, this uncontrolled extracellular magnetite formation results from the export of metabolic byproducts into the surrounding environment. Therefore, external environmental parameters such as the pH and Eh can greatly affect mineral formation.

Magnetite can also form through biologically controlled mineralization (BCM; Lowenstam 1981; Mann 1986). In BCM, minerals are deposited on or within organic matrices or vesicles inside the cell, allowing the organism to exert a high degree of control over the composition, size, habit, and intracellular location of the mineral. Because the intracellular pH and Eh are strongly controlled by the organism, mineral formation is not as affected by external environmental parameters as in BIM. Magnetite particles formed through BCM by the magnetotactic bacteria (the subject of this paper), are produced intracellularly, occur as well-ordered crystals, have a narrow size distribution, and have well-defined, consistent morphologies (Bazylinski and Moskowitz 1997). Thus, minerals produced by BCM may conceivably have structural or morphological characteristics that are distinguishable from minerals produced by BIM or purely inorganic processes.

McKay et al. (1996) cited the morphological similarity of nanometer-scale magnetite and iron sulfides in the rims of carbonate inclusions in the Martian meteorite ALH84001 to BCM magnetite and iron sulfides in terrestrial magnetotactic bacteria as part of the evidence for ancient life on Mars. Claims that nanometer-scale magnetite particles recovered from modern and ancient sediments are of biological origin (Chang and Kirschvink 1989; Petersen et al. 1986; Akai et al. 1991) have been based primarily on similar comparisons to grains produced by contemporary bacteria.

* Current address: Département des Sciences de la Terre (CNRS-UMR 6524), Université Blaise Pascal, 5 rue Kessler, F-63038 Clermont-Ferrand, France. E-mail: devouard@opgc.univ-bpclermont.fr

0003–004X/98/1112–1387$05.00

Although a few studies have compared BCM to BIM magnetite (Sparks et al. 1990; Moskowitz et al. 1989), reliable criteria for distinguishing biogenic from nonbiogenic magnetite have not been developed. In the present study, we compare the structural characteristics of BCM magnetite produced by magnetotactic bacteria with nonbiogenic magnetite of similar mean size. We used several pure cultured strains of magnetotactic bacteria as well as one synthetic sample as an example of nonbiogenic magnetite. Our goals were to use these "model" samples to determine: (1) the extent to which crystal morphologies and sizes are characteristic of their origin; and (2) whether there might be distinctive microstructural features that permit the reliable identification of biogenic magnetite, especially when the chain arrangements characteristic of magnetotactic bacteria cannot be used because of the degradation of the organic matter of the microorganism.

The minerals were studied by conventional and high-resolution transmission electron microscopy (HRTEM) and selected-area electron diffraction (SAED). A companion paper presents a similar study of iron sulfide minerals in magnetotactic bacteria (Pósfai et al. 1998).

Magnetotactic bacteria

Magnetotactic bacteria are a morphologically and physiologically diverse group of motile, Gram-negative procaryotes ubiquitous in aquatic environments (Blakemore 1982; Bazylinski 1995). They include coccoid, rod-shaped, vibrioid, spirillar (helical), and even multicellular forms. Physiological forms include denitrifiers that are facultative anaerobes, obligate microaerophiles, and anaerobic sulfate-reducers (Bazylinski and Moskowitz 1997). Thus, there are likely many species of magnetotactic bacteria (Spring et al. 1992), although only several have been isolated in pure culture (Bazylinski 1995). Each bacterium contains magnetosomes (Balkwill et al. 1980), which are grains of magnetic minerals (Frankel et al. 1979) within intracellular membrane vesicles (Gorby et al. 1988). The magnetosomes are generally arranged in chains that are anchored within a bacterium by as yet unknown structural elements.

With a few exceptions (Bazylinski and Moskowitz 1997), the bacterial magnetite grains are typically 35 to 120 nm in diameter, i.e., within the permanent, single-magnetic-domain (SD) size range (Moskowitz 1995). Magnetostatic interactions between the grains in the magnetosome chain result in a permanent magnetic dipole approximately equal in magnitude to the sum of the individual grain moments (Frankel and Blakemore 1989). The chain dipole moment is sufficiently large so that the bacterium is oriented in the geomagnetic field as it swims (Frankel 1984). Because of the inclination of the geomagnetic field, orientation of the bacterium facilitates its finding and maintaining an optimal position in vertical chemical gradients (e.g., oxygen, sulfur) common in the water column or sediments (Frankel et al. 1997).

A marked feature of magnetite from magnetotactic bacteria is that, in addition to the roughly equidimensional shapes interpreted as cuboctahedral {100} + {111} habits (Figs. 1a and 2j), several seemingly non-isometric morphologies have been described (Matsuda et al. 1983; Mann et al. 1984); these include prismatic (Figs. 1b and 1c) and tooth-, bullet-, or arrowhead shapes (Mann et al. 1987a, 1987b; Bazylinski et al. 1993; Iida and Akai 1996). The shapes appear to be consistent within given species or strains (Meldrum et al. 1993a, 1993b), although some variations of shape and size can occur within single magnetosome chains (Bazylinski et al. 1994). Smaller and more rounded particles are common at one or both ends of the chains and were interpreted as "immature" crystals by Mann and Frankel (1989). These shapes have been studied by HRTEM, and models based on distorted habits of simple forms have been proposed (Mann et al. 1984; Meldrum et al. 1993b). Indications of the 3D morphology can also be derived from thickness fringes visible on some thick crystals (Fig. 1d).

Magnetite and other spinel minerals are described in the *Fd3m* space group. Macroscopic crystals display octahedral {111}, more rarely dodecahedral {110}, or cubic {100} habits. Other forms are rare and appear as small truncations on one of the simpler forms (Goldschmidt 1918; Palache et al. 1944). Elongated growth can occur from the anisotropic development of equivalent faces, either because of anisotropy in the growth environment (such as flow or diffusion preferentially along certain directions) or anisotropy of the growth sites, typically caused by the presence of screw dislocations (Sunagawa 1987). In the case of magnetosomes, the anisotropy of the environment could derive from an anisotropic flux of ions through the magnetosome membrane surrounding the crystal (Gorby et al. 1988). The resulting crystals are distorted in a consistent species-specific manner. Magnetite crystals with elongated habits can be various combinations of the octahedron, cube, and dodecahedron (Fig. 2). Some of these habits have been referred to as "hexagonal prisms" (e.g., Mann and Frankel 1989; Sparks et al. 1990; Meldrum et al. 1993b), a terminology that should be avoided because it is both inconsistent with *Fd3m* symmetry and unnecessary.

Experimental methods

Magnetite grains in several cultured strains of magnetotactic bacteria were examined. These included the freshwater spirillum, *Magnetospirillum magnetotacticum,* and four incompletely characterized marine strains designated MV-1, MC-1, MC-2, and MV-4. MC-2 is a newly isolated, previously unreported microorganism; others have already been studied by various authors (Meldrum et al. 1993a, 1993b; Frankel et al. 1997; Bazylinski and Moskowitz 1997). We focused on these specific cultured strains because they provide pure samples of bacterial magnetite in various shapes and sizes.

M. magnetotacticum was grown in liquid culture as described by Frankel et al. (1997) under a microaerobic headspace gas mixture of 1% oxygen and 99% nitrogen, which is the optimal oxygen concentration for magnetite

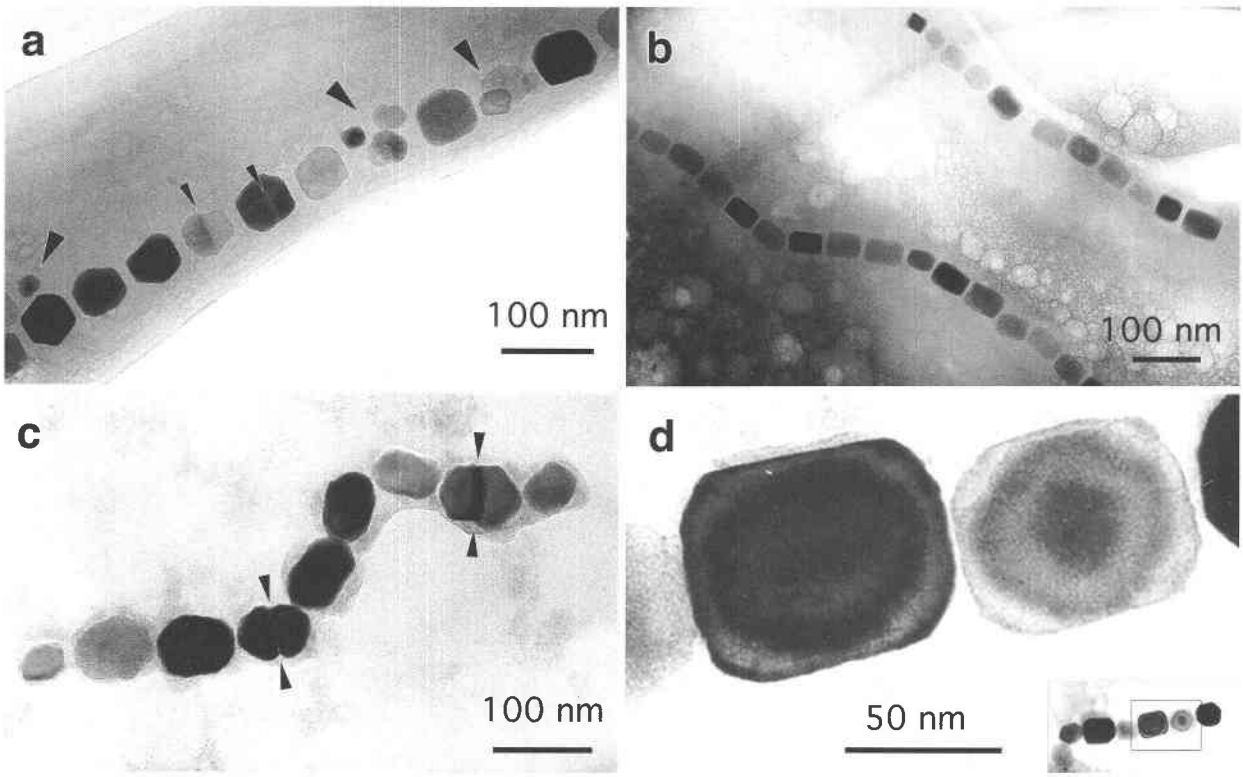

FIGURE 1. Low-magnification TEM micrographs of chains of magnetosomes, showing various morphologies. (**a**) Cuboctahedral crystals, twinned crystals (small arrows), and clusters of small crystals (large arrows) in *M. magnetotacticum*. (**b**) Rectangular crystals in strain MV-1. (**c**) Elongated crystals, some with re-entrant angles characteristic of twinning (arrowed), in strain MV-4; (**d**) Rectangular crystals with thickness fringes in strain MC-1.

formation (Blakemore et al. 1985). Strain MV-1, a vibrio that possesses a single polar flagellum, was grown anaerobically in a diluted, artificial seawater medium (Bazylinski et al. 1994) with nitrous oxide (N_2O) as the terminal electron acceptor; succinate and CasAmino Acids (a commercially available amino acid mix; Difco, Detroit, Michigan) were the organic carbon sources (Bazylinski et al. 1988). Strains MC-1 and MV-4 are microaerophilic (requiring only low amounts of oxygen for growth), bilophotrichous (possessing two flagellar bundles on one side of the cell) cocci and bipolarly flagellated spirilla, respectively. Cells of these strains were grown in semi-solid oxygen-gradient tubes in a diluted artificial seawater medium containing 10 m*M* thiosulfate as the energy source and sodium bicarbonate as the sole carbon source (Meldrum et al. 1993a, 1993b). There were no organic carbon sources in this medium, and thus these strains grew chemolithoautotrophically using inorganic energy (thiosulfate) and carbon (bicarbonate-carbon dioxide) sources. The headspace of these tubes was air. Cells formed flattened bands in these tubes at their preferred oxygen concentration somewhere below the meniscus of the growth medium. Strain MC-2 is a coccoid strain that was isolated recently from brackish water and mud collected from School Street Marsh, Woods Hole, Massachusetts, U.S.A. Cells of strain MC-2 are virtually identical to those of strain MC-1 and were grown similarly.

For all strains, samples of whole cells were prepared for electron microscopy by deposition of a drop of growth medium containing the bacteria onto a copper TEM mesh grid covered with a carbon film; after 15 s, the drop was removed and the grid was allowed to dry. In addition to the whole-cell samples, purified magnetite grains from strains MV-1 and *M. magnetotacticum* were obtained by incubating the bacteria in distilled water, causing the cells to burst from osmotic shock. The magnetosomes were then separated magnetically from the cell debris and treated with sodium hypochlorite to remove the magnetosome membranes and remaining cell debris. The magnetite grains were concentrated magnetically, rinsed several times with distilled water, and deposited onto TEM grids.

Synthetic magnetite grains were prepared in a reaction vessel by mixing aqueous solutions of $FeSO_4 \cdot 7H_2O$ and KNO_3 + KOH (Schwertmann and Cornell 1991). Oxygen was excluded by using an air-tight rubber plug and continuous Ar flow through the vessel. The mixed solutions were heated for ~50 min at 85 °C while stirring and then allowed to cool overnight.

All bacterial samples were kept frozen until TEM examination to avoid possible modification by dissolution,

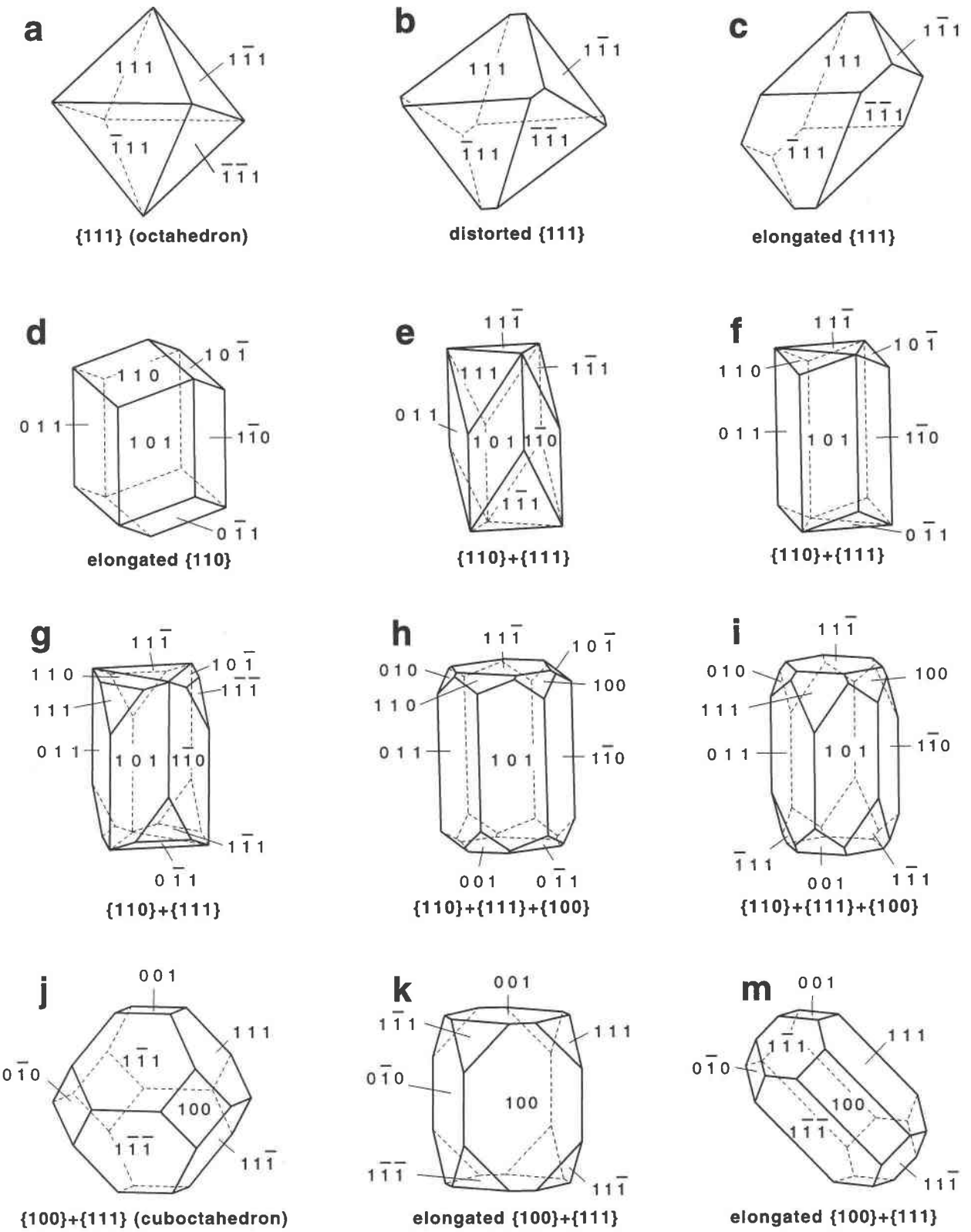

FIGURE 2. Combinations of forms compatible with magnetite (*Fd3m*) symmetry. The cube {100}, octahedron {111}, and dodecahedron {110} can, if appropriately distorted, produce a wide range of shapes accounting for those observed in magnetosomes.

recrystallization, or oxidation. TEM observations were conducted on various microscopes: JEOL JEM-4000ex, JEM-2000fx, and Topcon 002B TEMs, operated at 400, 200, and 200 keV, respectively. SAED patterns were obtained from some crystals, but the small sizes of individual crystals compared to the smallest selected-area aperture meant that many SAED patterns were complicated by reflections from nearby crystals.

Results

Bacterial magnetite

Statistical analysis of sizes and shapes. To quantify the size and shape distributions of bacterial magnetites, we performed statistical analyses of sizes of particles from *M. magnetotacticum* and strains MV-1 and MC-2 (Fig. 3). Crystal outlines were digitized from scanned, low-magnification TEM photomicrographs and their dimensions estimated by calculating the best fit of an ellipse (of same surface) to the contours. The length (L) and width (W) of a crystal were then matched to the major and minor axes, respectively, of the best-fitting ellipse. This type of analysis allowed a quantification of sizes and elongations that might be difficult to measure objectively when dealing with certain shapes. That is, whereas the distinction between L and W of a rectangle is readily evident (although the longest dimension is not the length but the diagonal), the notion of L and W is not as clear for diamond shapes or polygons. The sizes reported in Figure 3 are the averages of L and W; the shape factors, describing the elongation of the crystals, were chosen as the ratio W/L (<1). Although this ellipse-fitting method can introduce differences from actual measurements of L and W, the differences were checked and found to have negligible effects on the distributions, even though the absolute mean values can differ somewhat from published results obtained with other methods (Meldrum et al. 1993b).

Figure 3 shows that the sizes of magnetite crystals from magnetotactic bacterial strains *M. magnetotacticum* and MV-1 are distributed over a narrow range; MC-2 crystals are larger and have a somewhat broader size distribution. The distributions from all three strains are asymmetric, with sharp cut-offs toward larger sizes. There is overlap of the size distributions for different strains, but the mean sizes clearly differ.

The shape-factor analyses for magnetite crystals of *M. magnetotacticum* and strain MC-2 show distributions bounded by one, with maxima around 0.85. The fact that the maxima are not closer to one, as expected for truly isometric shapes, is probably the result of a combination of minor distortions, measurement errors, and the fact that the projection of a regular cuboctahedron along a random direction has a shape factor smaller than one. For strain MV-1, which has elongated magnetosomes, the shape factor has a maximum frequency around 0.65. The distribution is asymmetric, with a cut-off toward the small values corresponding to the maximum elongations of the crystals. The distribution decreases toward one as a consequence of both the presence of rounded, presumably immature crystals and the measurement of crystals seen along projections not perpendicular to the elongation axis.

Defects and twinning. Bacterial magnetite has been reported to be of high structural perfection (Bazylinski et al. 1994; Meldrum et al. 1993a, 1993b). Figure 4 shows a typical crystal free of extended defects. In particular, no dislocation lines are observed along the direction of elongation of the distorted crystals, which suggests a screw dislocation model is an unlikely explanation for the anisotropy of these crystals. We used HRTEM to characterize the microstructures of bacterial magnetite, focusing on twinning such as was reported by Mann and Frankel (1989) and Iida and Akai (1996).

Although most bacterial magnetite crystals are free of imperfections, twinned crystals were observed in all five studied bacterial strains. The frequency of such crystals varies from strain to strain as shown in Table 1, and could be as high as 40% for MV-4. The proportion of twinned crystals also seems to be significantly higher in some individual cells within a given strain. In addition to twinning, a few defects that could be stacking faults (Fig. 5a) or sub-grain boundaries were observed.

All twinned crystals that could be characterized by HRTEM show that the individuals are related by rotations of 180° around the [111] direction, with a common (111) contact plane, i.e., they obey the spinel twin law, which is the most common twin mechanism of magnetite (Palache et al. 1944; Chen et al. 1982). Such twinning does not necessarily affect the magnetization of the crystals because the easy axis of magnetization in magnetite is $<111>$, i.e., the common direction of the twin (Mann and Frankel 1989).

Moiré interference fringes are commonly observed at the contact between twinned individuals seen along the [110] zone axis (Fig. 5b). Because the (111) twin plane is parallel to this direction of observation, moiré effects that result from overlapping twin individuals indicate that the contact surface is irregular rather than a straight (111) plane. The interpretation as a moiré effect rather than a superstructure is straightforward in the rare cases where the perimeters of individual crystals are clearly visible (Fig. 5b). In other cases, it can be determined by the numerical addition of structure images from the two individuals (Fig. 5c), which produces a periodic contrast similar to that observed at the twin boundary.

Figure 6 shows multiple twins related by the spinel twin law. As for some simple twins, the contact planes are irregular and display moiré fringes. The diffraction pattern (Fig. 6c) and interpretative sketch (Fig. 6b) show the two twin planes corresponding to a pair of octahedral faces such as (111) and $(\bar{1}\bar{1}1)$. Such a cyclic triplet has a closure gap between crystals 2 and 3 (Fig. 6) making a dihedral angle of about 33°. This gap can be healed by lateral growth of the crystals, creating a disordered grain boundary, which is visible near the broad arrow in Figure 6a. In this case, the easy directions of magnetization of

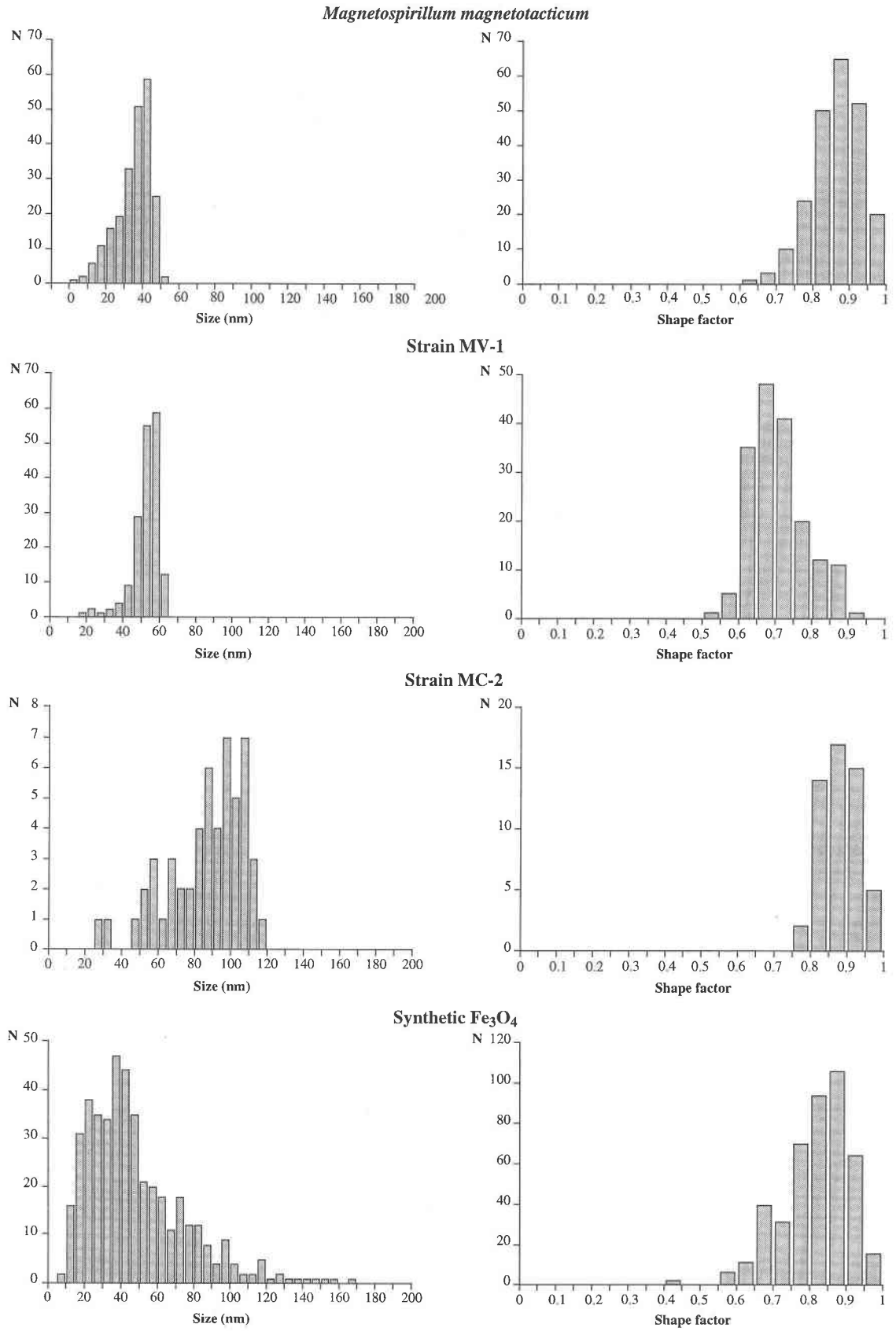

FIGURE 3. Size and shape distributions for bacterial (*M. magnetotacticum* and strains MV-1 and MC-2) and synthetic magnetite.

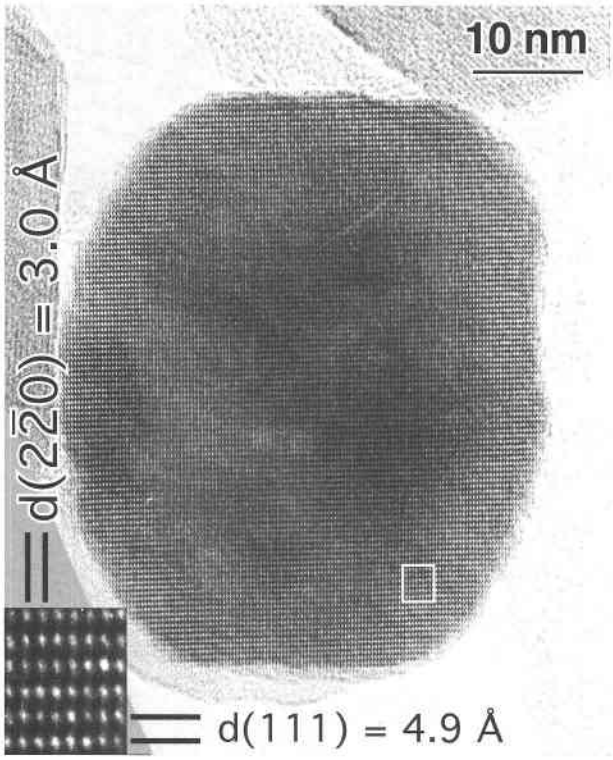

FIGURE 4. High-resolution image of a typical unfaulted magnetite crystal in [11$\bar{2}$] projection. The boxed area is enlarged in the inset (*M. magnetotacticum*).

TABLE 1. Estimated percentages of twinned crystals from various strains of bacteria and from a synthetic sample

	Twins (%)	Multiple twins (%)
M. magnetotacticum	10 to 20	4
Strain MV-1	6 to 8	1
Strain MV-4	34 to 45	18
Strain MC-1	2 to 7	1
Strain MC-2	11 to 16	3
Synthetic Fe_3O_4	11 to 17	4

Notes: Over 120 crystals were observed for each type (except strain MC-2, for which 62 were counted). The proportion of twins (second column) includes multiple twins. These estimations should be considered as approximate, because only low-magnification images were used and it is difficult to detect twinning when the crystals are not close to Bragg orientation. Also, some of the reported twins might be grain boundaries. Ranges reflect the uncertainty as well as variations between chains of magnetosomes.

the three crystals are no longer collinear, suggesting that the microorganism can tolerate some fraction of magnetosomes that are not single magnetic domains.

As with sizes and morphologies, the characteristics of twins are somewhat species-specific. For example, in strain MV-1 most twinned crystals have planar contact surfaces and euhedral shapes (Fig. 5a), whereas in *M. magnetotacticum* and strain MC-2, the twin surfaces are more irregular, and the twinned grains tend to have globular shapes (Figs. 1a, 6a, and 6d); in strain MV-4, many twinned crystals have a characteristic "waisted" aspect (Fig. 1c).

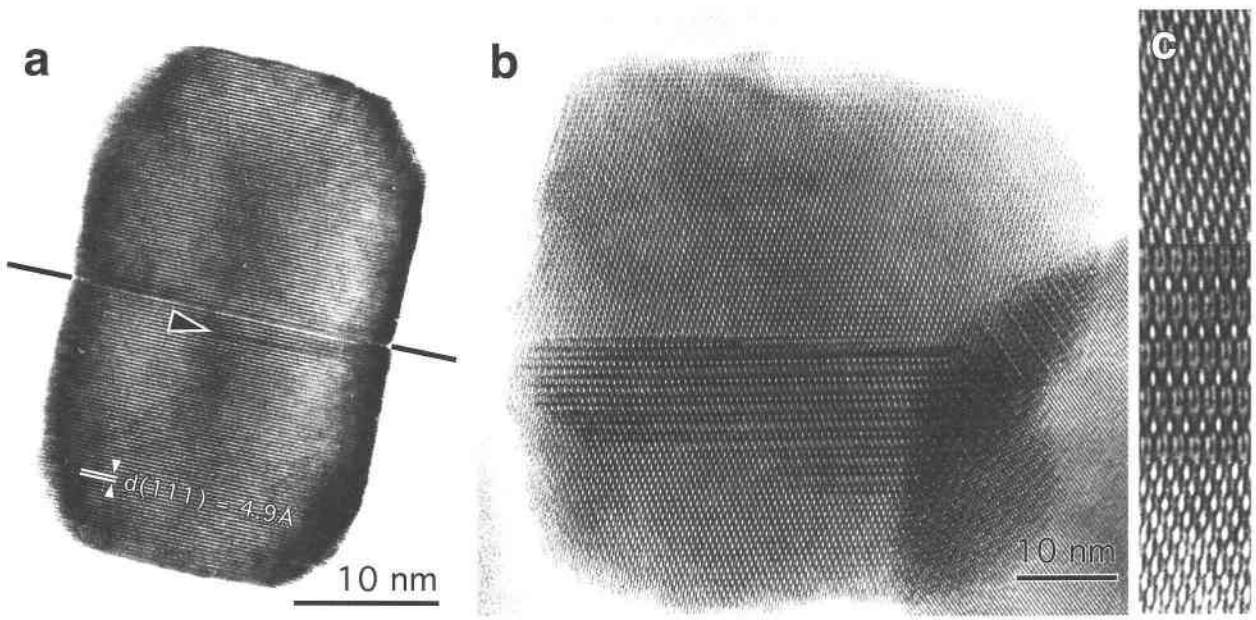

FIGURE 5. High-resolution images of simple twins in bacterial magnetite. (**a**) Twin with a straight contact plane and a linear contrast feature (arrowed) that can be interpreted as a stacking fault (MV-1). (**b**) Twinned crystals with an irregular twin plane leading to a moiré effect where the two crystals overlap (*M. magnetotacticum*). (**c**) The numerical summation of portions of the structure images from top and bottom crystals in (b) results in a moiré pattern (enlarged) with identical periodicity and a contrast similar to that in (b).

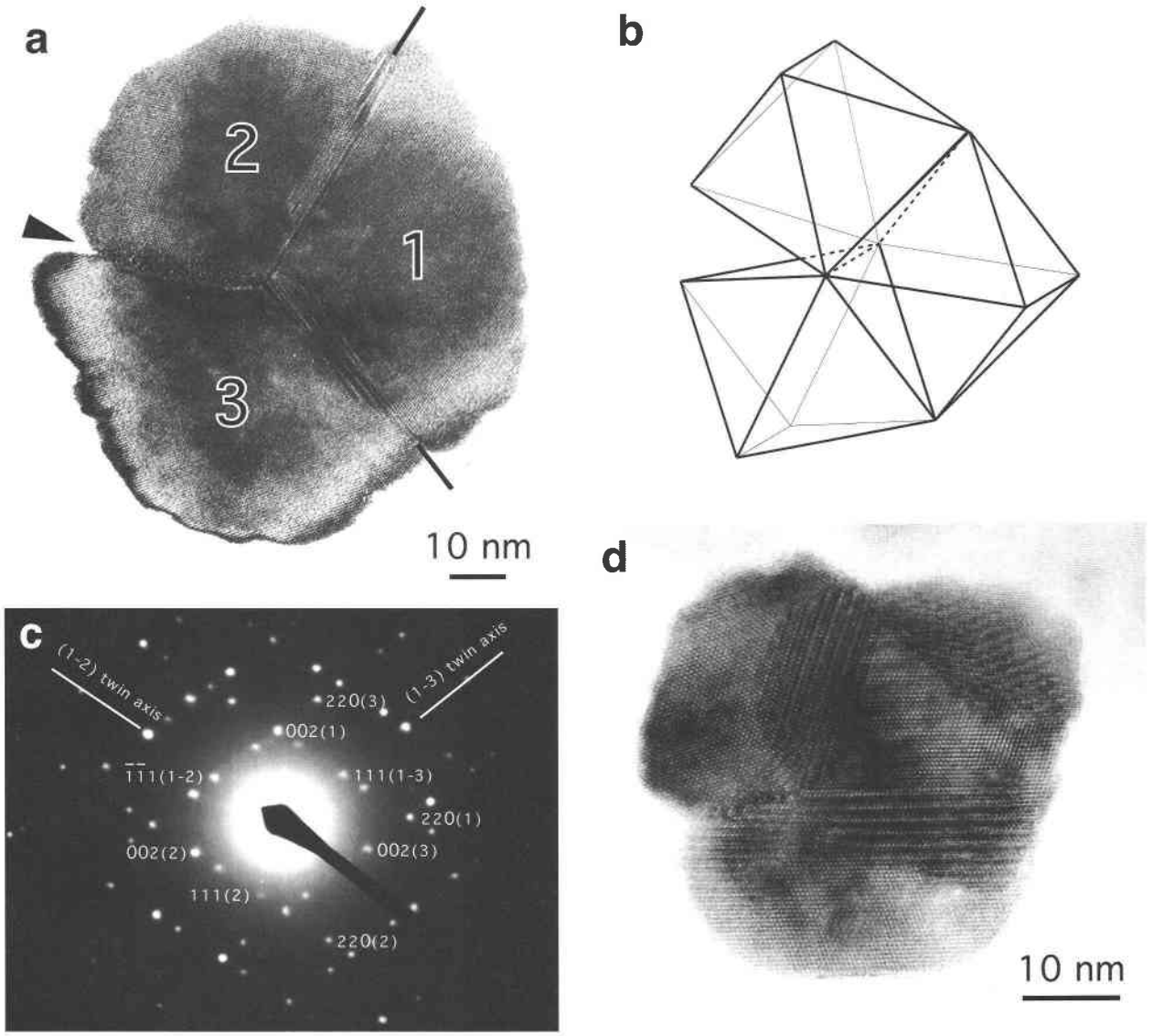

FIGURE 6. Multiple twins in bacterial magnetite. (**a**) Cyclic twin (strain MC-2). Twin boundaries between crystals 1 and 2, and 1 and 3 are stepped, whereas the contact between 2 and 3 is an irregular grain boundary (arrowed). (**b**) Interpretative scheme of the twinning of three regular octahedra as in (a), showing the large closure gap between crystals 2 and 3. (**c**) Indexed diffraction pattern from the triplet in (a). Numbers following the indices between parentheses refer to the crystal number, as labeled above. (**d**) Multiple twin from *M. magnetotacticum.*

Synthetic magnetite

Although the synthetic magnetite crystals prepared in this study are not representative of all types of nonbiogenic magnetite, natural or synthetic, they present a useful starting point for comparison with biogenic crystals in the same size range.

TEM observations of the synthetic magnetite show well-formed octahedral crystals (Fig. 7). An obvious difference from the bacterial samples is that the crystals have better defined crystal faces and sharper corners, but such angularity is not a reliable criterion because minor variations of morphologies can be expected from various types of nonbiogenic samples. The size distribution of our synthetic crystals (Fig. 3) shows that most crystals are in the SD size range, and their mean size is comparable to that of magnetites from magnetotactic bacteria. However, the asymmetry of the size distribution is opposite to that of the bacterial samples, with a "tail" of larger crystals up to 170 nm. The shape-factor distribution is similar to that of *M. magnetotacticum* and strain MC-2. As discussed for *M. magnetotacticum,* shape factors smaller than one can be explained by the various projections of the octahedra and also by the presence of less isometric twinned crystals (see below).

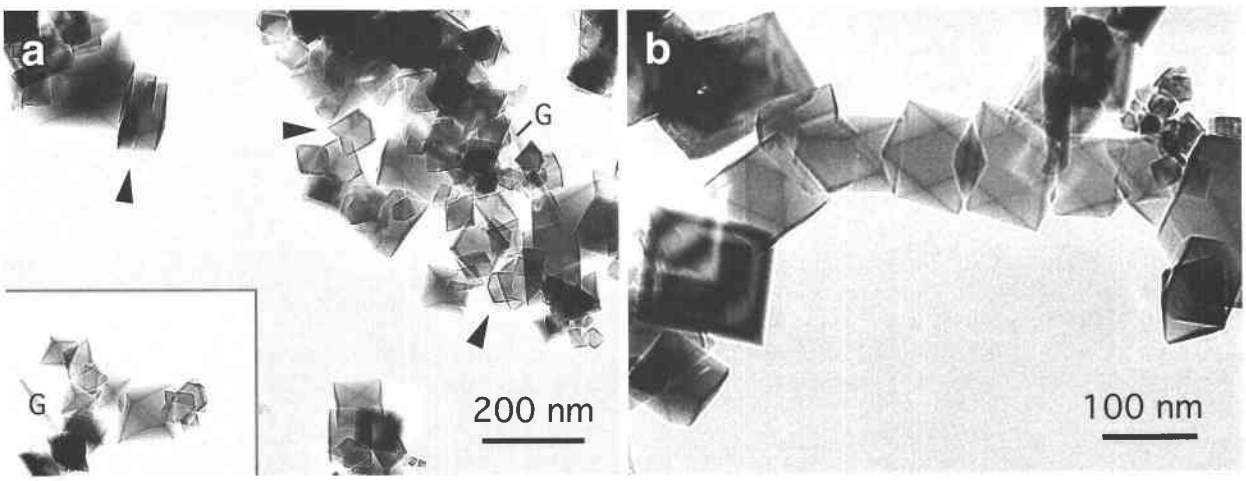

FIGURE 7. Low-magnification TEM micrographs of synthetic magnetite. (**a**) Typical aggregates showing slightly distorted octahedral morphologies, the wide range of sizes, and a few twinned crystals (arrowed). The needle-shaped crystals (G) are goethite. (**b**) A small chain of octahedra, some of which share {111} faces.

Low-magnification images show some crystals in chain-like configurations with a common [111] direction (Fig. 7b). However, the equilibrium configuration is not chain-like but an approximately random aggregate (Fig. 7a).

Crystals twinned according to the spinel law also occur in the synthetic sample and show two extreme shapes: (a) Twins associating two octahedra flattened in the direction perpendicular to the twin plane (Fig. 7a and 8a); the resulting sparrow-tail morphology is common for macroscopic twins of spinel and other isometric minerals such as diamond (Sunagawa 1987). (b) Twinned crystals formed by two octahedra sharing all or part of a triangular (111) face, but with both individuals retaining their regular octahedral morphology (Fig. 8b). All variations of cases a and b were observed, including twins of octahedra of different sizes.

Contact planes of many twinned crystals are straight [as for case a, shown in Figure 8b], but stepped or irregular contact surfaces leading to moiré patterns also occur (Fig. 8c), as in the bacterial magnetite crystals.

Mottled contrast can be seen in some high-resolution images and is associated with diffuse streaks in the diffraction patterns (Fig. 8a). This phenomenon appeared only after prolonged observation of the same crystal and can be attributed to beam damage, probably reduction of Fe^{3+} to Fe^{2+} caused by the 400 keV electron beam.

DISCUSSION AND CONCLUSIONS

Bradley et al. (1996) reported elongated magnetite crystals with indications of central screw dislocations in the Martian meteorite ALH84001. They interpreted these as evidence for a whisker-type growth mechanism, typical of vapor-grown crystals at high temperatures and hence inconsistent with biological activity. The HRTEM investigation of magnetite crystals from five strains of magnetotactic bacteria confirms earlier observations that most bacterial crystals contain no extended defects. In particular, no screw dislocations were observed. But since our synthetic magnetite crystals of similar size also lack dislocations, structural perfection cannot be considered a reliable criterion for distinguishing biogenic from nonbiogenic magnetite. Bradley et al. (1996) also reported twinned magnetite crystals in ALH 84001 and used such twins as further evidence of a nonbiogenic origin. We found that twinning according to the spinel law is a reasonably common feature of bacterial as well as synthetic magnetite crystals.

There is no indication that twinning of bacterial magnetite could be the result of a phase transition or of external strains, conditions that can produce twins. We therefore assume the twinning is a growth phenomenon. In the twinned bacterial crystals, both individuals are developed roughly equally, suggesting that they nucleated more or less simultaneously. However, the common irregularity of the twin planes suggests two separate crystal surfaces growing into contact rather than growth of an early twinned nucleus. In the synthetic sample, flattened twins with sparrow-tail morphology are typical of twinning that occurred soon after nucleation, with growth of the two crystals affected equally by the twinning. The flattening is primarily the result of the fact that the faces constituting the twin plane cannot grow anymore. Reentrant edges and twin junctions provide additional growth sites, promoting the extension of the twin along the twin plane (Sunagawa 1987). However, twins associating individuals with regular octahedral morphologies are difficult to explain by this mechanism and might represent a case of crystallographically controlled juxtaposition, in which the two crystals nucleate and grow to their regular morphologies before coming into contact. Such a mechanism would result from the permanent magnetization of SD-sized nanocrystals of magnetite, which can orient one another in approximate twin positions, driven by their

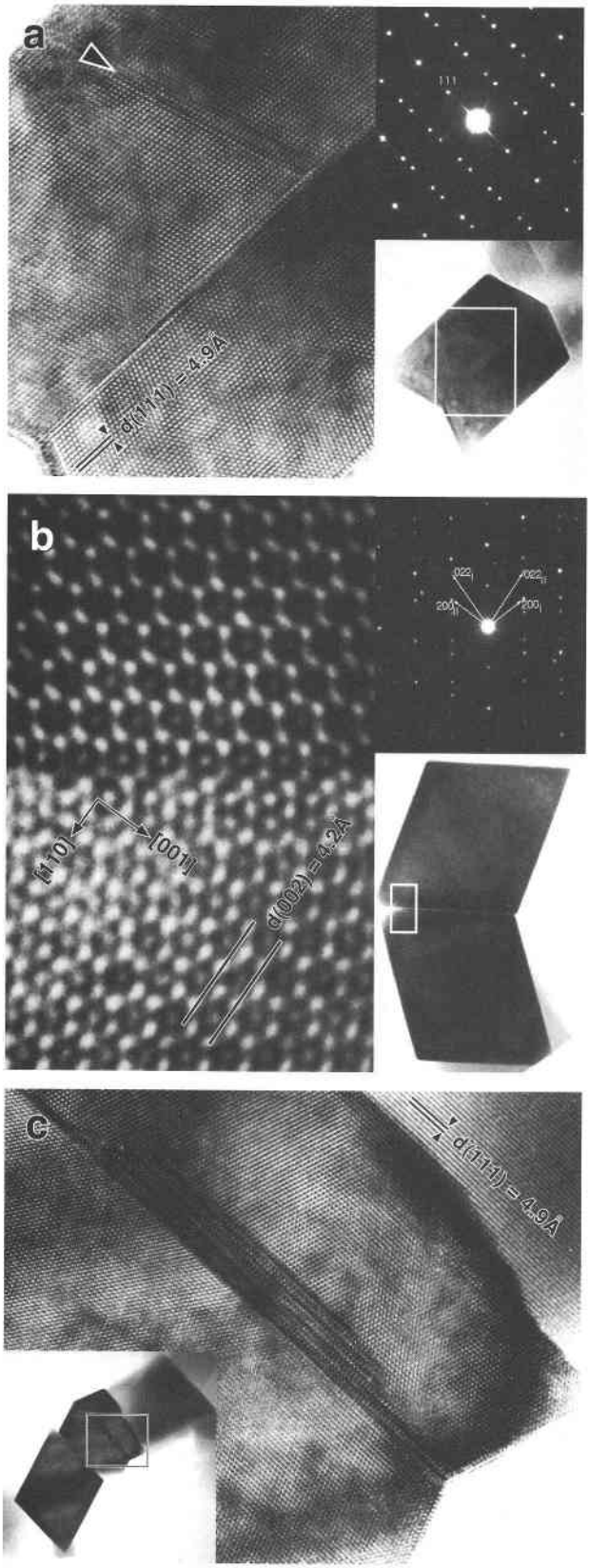

FIGURE 8. TEM micrographs of spinel-law twins in synthetic magnetite. (**a**) Typical flat twin. Inserts: diffraction pattern and low-magnification images (the framed area is enlarged on the left). In addition to twinning, a thin strip of stacking faults is visible (arrowed). (**b**) Twinning of two regular octahedra. Inserts: diffraction pattern and low-magnification image (the framed area is enlarged on the left). (**c**) Three crystals with parallel (111) planes, one of them twinned. From left to right (low-magnification picture in insert): a regular octahedron and a flat twin are seen along the same [110] zone, but the third crystal is rotated around the common [111] direction, as indicated by the fringe contrast.
←

magnetic moments. The final orientation to a perfect twin position (around the common [111] direction) minimizes the interface energy, but might be partly serendipitous. Figure 8c shows such crystals sharing common (111) faces; although the two lower-left crystals are both in [110] zone-axis orientations, i.e., in perfect twin position, the lattice fringes in the topmost crystal indicate that it is noticeably disoriented from the twin orientation. Flat, stepped, and irregular twin boundaries were observed in both biogenic and nonbiogenic magnetite, and thus twinning should not be used to distinguish the origin of small magnetite crystals.

It seems that sparse assemblages of a few crystals in chain-like configurations are also not conclusive, since short chains were found in the synthetic magnetite sample. Such arrangements can be explained by the fact that SD crystals are permanent magnets and could tend to form short chains in solution. It is conceivable that these chain-like configurations in the nonbiogenic magnetite preparations could be an artifact of preparation (e.g., during drying of the solution). However, we consider it more probable that they indeed occurred in the solution, where the magnetic driving force was more likely to affect the arrangement of the grains. It remains to be determined whether similar chains can occur nonbiogenically in the geological environment.

Statistical analysis of bacterial magnetite crystals from magnetosomes show narrow asymmetric size distributions and consistent W/L ratios within individual species, whereas synthetic magnetite crystals of similar mean size are distinctively different and have a size distribution that extends to relatively large crystals. The statistical analysis reflects the control of the bacteria, which limits the growth of the magnetite crystals to specific sizes and morphologies, as marked by the asymmetry of the size and shape distributions for strain MV-1. Statistical analysis of sizes and shapes might provide robust criteria for distinguishing between biogenic (BCM type) and nonbiogenic magnetic crystals, for the following reasons: (1) the synthetic magnetite could be distinguished from bacterial magnetite, despite the fact that the former was prepared by rapid precipitation from an aqueous solution, a process known to produce small crystals of homogeneous size distributions, i.e., with characteristics close to those

expected for biomagnetites; and (2) although the distortion of isometric crystals to elongated growth habits is not uncommon within nonbiogenic magnetites, a large number of crystals showing identical distortions would require steady growth conditions that are seldom attained in natural nonbiogenic or synthetic environments. It is difficult to conceive of a nonbiologically controlled mechanism that could produce shape distributions with sharp cut-offs at particular low axial ratios, as depicted in Figure 3. Vapor-grown crystals of magnetite (synthetic or from volcanic fumaroles) can form elongated crystals and needles by a mechanism involving axial screw dislocations (Bradley et al. 1996). However, the growth of such whiskers is unconstrained, and shape distributions similar to those of the elongated crystals produced by BCM would not be expected.

Additional statistical analysis of various bacterial and nonbiogenic samples should be performed to extend the results of this study from model samples to more complex natural cases. Additional factors that could impede distinguishing between bio- and nonbiogenic magnetite crystals by size and shape analysis are the mixing of different species of magnetotactic organisms in the same deposit as well as subsequent modifications of crystals caused by dissolution, reprecipitation, or Ostwald ripening. The case of bacterial iron sulfides is yet more complicated because of possible structural variations. This is the object of the companion paper by Pósfai et al. (1998).

Acknowledgments

This research was supported by NSF grant CHE 9714101 and NASA grant NAG5-5118. The electron microscopy was performed in the Center for High Resolution Electron Microscopy at Arizona State University. Additional TEM work was performed at the CRMC2-CNRS facility in Marseille, France. Reviews by D.A. Brown, B.L. Sherriff, and an anonymous reviewer improved the manuscript, as did comments from J. Banfield.

References cited

Akai, J., Sato, T., and Okusa, S. (1991) TEM study on biogenic magnetite in deep-sea sediments from the Japan Sea and the Western Pacific Ocean. Journal of Electron Microscopy, 40, 110–117.

Balkwill, D.L., Maratea, D., and Blakemore, R.P. (1980) Ultrastructure of a magnetic spirillum. Journal of Bacteriology, 141, 1399–1408.

Banfield, J.F. and Nealson, K.H. (1997) Geomicrobiology: Interactions between microbes and minerals. In Mineralogical Society of America Reviews in Mineralogy, 35, 448.

Bazylinski, D.A. (1995) Structure and function of the bacterial magnetosome. ASM News, 61, 337–343.

Bazylinski, D.A. and Moskowitz, B.M. (1997) Microbial biomineralization of magnetic iron minerals. In Mineralogical Society of America Reviews in Mineralogy, 35, 181–223.

Bazylinski, D.A., Frankel, R.B., and Jannasch, H.W. (1988) Anaerobic magnetite production by a marine magnetotactic bacterium. Nature, 334, 518–519.

Bazylinski, D.A., Heywood, B.R., Mann, S., and Frankel, R.B. (1993) Fe_3O_4 and Fe_3S_4 in a bacterium. Nature, 366, 218.

Bazylinski, D.A., Garratt-Reed, A.J., and Frankel, R.B. (1994) Electron microscopic studies of magnetosomes in magnetotactic bacteria. Microscopy Research and Technique, 27, 389–401.

Blakemore, R.P. (1982) Magnetotactic bacteria. Annual Reviews in Microbiology, 36, 217–238.

Blakemore, R.P., Short, K.A., Bazylinski, D.A., Rosenblatt, C., and Frankel, R.P. (1985). Microaerobic conditions are required for magnetite formation within *Aquaspirillum magnetotacticum*. Geomicrobiology Journal, 4, 53–71.

Bradley, J.P., Harvey, R.P., and McSween, H.Y. Jr. (1996) Magnetite whiskers and platelets in the ALH84001 Martian meteorite: Evidence of vapor phase growth. Geochimica et Cosmochimica Acta, 60, 5149–5155.

Chang, S.-B. and Kirschvink, J.L. (1989) Magnetofossils, the magnetization of sediments, and the evolution of magnetite biomineralization. Annual Review of Earth and Planetary Sciences, 17, 169–195.

Chen, K., Sun, D., Wang, Z., Yang, T., and Liu, W. (1982) The genetic significance of magnetite twins from China. Bulletin de Minéralogie, 105, 11–19.

Frankel, R.B. (1984) Magnetic guidance of organisms. Annual Reviews in Biophysics and Bioengineering, 13, 85–103.

Frankel, R.B. and Blakemore, R.P. (1989) Magnetite and magnetotaxis in microorganisms. Bioelectromagnetics, 10, 223–237.

Frankel, R.B., Blakemore, R.P., and Wolfe, R.S. (1979) Magnetite in freshwater magnetotactic bacteria. Science, 203, 1355–1356.

Frankel, R.B., Bazylinski, D.A., Johnson, M.S., and Taylor, B.L. (1997) Magneto-aerotaxis in marine coccoid bacteria. Biophysical Journal, 73, 994–1000.

Goldschmidt, V. (1918) Atlas der Kristallformen, Heidelberg.

Gorby, Y.A., Beveridge, T.J., and Blakemore, R.P. (1988) Characterization of the bacterial magnetosome membrane. Journal of Bacteriology, 170, 834–841.

Iida, A. and Akai, J. (1996) TEM study on magnetotactic bacteria and contained magnetite grains as biogenic minerals, mainly from Hokuriku-Niigata region, Japan. Science Reports of Niigata University, Series E (Geology), 11, 43–66.

Lovley, D.R. (1991) Dissimilatory Fe(III) and Mn(IV) reduction. Microbiological Reviews, 55, 259–287.

Lowenstam, H.A. (1981) Minerals formed by organisms. Science, 211, 1126–1131.

Lowenstam, H.A. and Weiner, S. (1989) On biomineralization, 324 p. Oxford University Press, Oxford, New York.

Mann, S. (1986) On the nature of boundary-organized biomineralization. Journal of Inorganic Chemistry, 28, 363–371.

Mann, S. and Frankel, R.B. (1989) Magnetite biomineralization in unicellular organisms. In S. Mann, J. Webb, and R.J.P. Williams, Eds., Biomineralization: Chemical and biochemical perspectives, p. 389–426. VCH Publishers, New York.

Mann, S., Moench, T.T., and Williams, R.J.P. (1984) A high resolution electron microscopic investigation of bacterial magnetite. Implications for crystal growth. Proceedings of the Royal Society of London B, 221, 385–393.

Mann, S., Sparks, N.H.C., and Blakemore, R.P. (1987a) Ultrastructure and characterization of anisotropic inclusions in magnetotactic bacteria. Proceedings of the Royal Society of London B, 231, 469–476.

——— (1987b) Structure, morphology and crystal growth of anisotropic magnetite crystals in magnetotactic bacteria. Proceedings of the Royal Society of London B, 231, 477–487.

Matsuda, T., Endo, J., Osakabe, N., and Tonomura, A. (1983) Morphology and structure of biogenic magnetite particles. Nature, 302, 411–412.

McKay, D.S., Gibson, E.K. Jr., Thomas-Keprta, K.L., Vali, H., Romanek, C.S., Clemett, S.J., Chillier, X.D.F., Maechling, C.R., and Zare, R.N. (1996) Search for past life on Mars: Possible relic biogenic activity in Martian meteorite ALH84001. Science, 273, 924–930.

Meldrum, F.C., Mann, S., Heywood, B.R., Frankel, R.B., and Bazylinski, D.A. (1993a) Electron microscopy study of magnetosomes in a cultured coccoid magnetotactic bacterium. Proceedings of the Royal Society of London B, 251, 231–236.

——— (1993b) Electron microscopy study of magnetosomes in two cultured vibrioid magnetotactic bacteria. Proceedings of the Royal Society of London B, 251, 237–242.

Moskowitz, B.M. (1995) Biomineralization of magnetic minerals. Reviews in Geophysics Supplementum, 123–128.

Moskowitz, B.M., Frankel, R.B., Bazylinski, D.A., Jannasch, H.W., and Lovley, D.R. (1989) A comparison of magnetite particles produced anaerobically by magnetotactic and dissimilatory iron-reducing bacteria. Geophysical Research Letters, 16, 665–668.

Palache, C., Berman, H., and Frondel, C. (1944) Dana's system of mineralogy, 384 p. Wiley, New York.

Petersen, N., Von Dobeneck, T., and Vali, H. (1986) Fossil bacterial magnetite in deep-sea sediments from the South Atlantic Ocean. Nature, 320, 611–615.

Pósfai, M., Buseck, P.R., Bazylinski, D.A., and Frankel, R.B. (1998) Iron sulfides from magnetotactic bacteria: Structure, composition, and phase transitions. American Mineralogist, 83, 1467–1479.

Schwertmann, U. and Cornell, R.M. (1991) Iron oxides in the laboratory: preparation and characterization, 137 p. Weinheim, New York.

Sparks, N.H.C., Mann, S., Bazylinski, D.A., Lovley, D.R., Jannasch, H.W., and Frankel, R.B. (1990) Structure and morphology of magnetite anaerobically-produced by a marine magnetotactic bacterium and a dissimilatory iron-reducing bacterium. Earth and Planetary Science Letters, 98, 14–22.

Spring, S., Amann, R., Ludwig, W., Schleifer, K.-H., and Petersen, N. (1992) Phylogenetic diversity and identification of non-culturable magnetotactic bacteria. Systematic and Applied Microbiology, 15, 116–122.

Sunagawa, I. (1987) Morphology of minerals. In I. Sunagawa, Ed., Morphology of crystals, p. 511–587. Terra Scientific Publishing, Tokyo.

Manuscript received March 9, 1998
Manuscript accepted August 18, 1998
Paper handled by Jillian F. Banfield

American Mineralogist, Volume 83, pages 1399–1408, 1998

Formation of Fe-silicates and Fe-oxides on bacterial surfaces in samples collected near hydrothermal vents on the Southern Explorer Ridge in the northeast Pacific Ocean

DANIELLE FORTIN,[1,*] F. GRANT FERRIS,[2] and STEVEN D. SCOTT[2]

[1]Department of Geology, University of Ottawa, Ottawa, Ontario, K1N 6N6, Canada
[2] Department of Geology, E.S.C., University of Toronto, Toronto, Ontario, M5S 3B1, Canada

ABSTRACT

Samples collected in low-temperature (2–50 °C) waters near hydrothermal vents of the Southern Explorer Ridge, in the northeast Pacific Ocean, contained fine (<500 nm) Fe- and Mn-oxide and Fe-silicate particles coating bacterial surfaces. Partially to totally mineralized bacteria, along with bacterial exopolymers, were covered with a mixture of poorly ordered Si-rich Fe-oxides (possibly ferrihydrite), Mn-oxides, and Fe-silicates (possibly nontronite). Minerals occur as very fine (2–20 nm) granular material, fine (20–100 nm) needles and sheets, small (200–500 nm) nodules and filaments (i.e., mineralized exopolymers). Under saturation conditions, we infer that bacterial surfaces provided nucleation sites for poorly ordered oxides and silicates. The formation of Fe- and Mn-oxides was likely initiated by the direct binding of soluble Fe and Mn species to reactive sites (like carboxyl, phosphate, and hydroxyl groups) present within the bacterial cell wall and the exopolymers. Fe-silicate formation involved a more complex binding mechanism, whereas metal ions, such as Fe, possibly bridged reactive sites within the cell walls to silicate anions to initiate silicate nucleation.

INTRODUCTION

Deep-sea hydrothermal vents associated with sea floor volcanism are found in many regions of the Atlantic and Pacific oceans as well as the Red Sea. As high-temperature, reducing, and acidic solutions mix with sea water, various minerals precipitate around the vents. The dominant minerals observed near hydrothermal vents are Fe-oxides (rich in Si and Mn) and Fe-sulfides, along with some sulfates, silicates, and carbonates (Juniper and Tebo 1995). Hydrothermal deposits can form not only at high temperatures near the vent openings, but also on the sea floor where the temperatures range from 2 to 50 °C (Juniper and Tebo 1995).

Hydrothermal sites are also a natural habitat for various microbial communities, such as free-living bacterial populations associated with discharged vent fluids, free-living microbial mats growing on rocks, chimneys, and sediments, endosymbiotic and exosymbiotic associations of microorganisms and vent fauna, and microorganisms within deep-sea hydrothermal vent plumes (Karl 1995). Microbial communities likely derive their energy from the oxidation of partially to fully reduced inorganic compounds, including Fe, Mn, and S, released by the vents (Karl 1995). However, no study to date has fully established a direct role (i.e., an enzymatically catalyzed reaction) for bacteria in the formation of Fe-oxides at hydrothermal vents (Juniper and Tebo 1995). Microbial Fe accumulation at these sites is therefore seen as an indirect mechanism, whereby bacteria trigger the chemical precipitation of Fe-oxides, by locally changing redox and/or pH conditions through their metabolic activity.

Bacteria can also act as nucleation surfaces for Fe-rich minerals. Bacterial surfaces can easily bind dissolved ionic species thereby leading to the nucleation of various minerals, such as oxides, silicates, carbonates, and sulfides (see review by Fortin et al. 1997). This happens because bacterial cell wall components possess amphoteric and amino groups that can sorb various ionic species, including metals (Beveridge 1981). Under solution saturation conditions, bacteria act as geochemically reactive solids (Mullen et al. 1989; Fein et al. 1997) and can, in some cases, increase the precipitation reaction rate (Fortin and Beveridge 1997).

The present study examines the morphology, chemistry, and mineralogy of Si- and Mn-rich iron oxides and Fe-silicates present in hydrothermal deposits collected near the Southern Explorer Ridge in the northeast Pacific ocean. Analyses of the deposit material by transmission electron microscopy (TEM) and energy dispersive X-ray spectroscopy (EDS) indicate that bacteria and their associated exopolymers served as nucleation surfaces for Fe-oxide and Fe-silicate formation.

EXPERIMENTAL DETAILS

Location

The present study was part of the CANRIDGE III investigation of ocean ridges, which is a part of the international InterRIDGE program. Samples were collected in

* E-mail: dfortin@science.uottawa.ca

0003–004X/98/1112–1399$05.00